Structural properties and biological activities of collagens from four main processing by-products (skin, fin, cartilage, notochord) of sturgeon *(Acipenser gueldenstaedti)*

Dawei Meng[a*], Qiwei Wei[b], Yasuaki Takagi[c], Zhiyuan Dai[a], Yan Zhang[d]

a Zhejiang Province Joint Key Laboratory of Aquatic Products Processing, Institute of Seafood, Zhejiang

Gongshang University, 149 JiaoGong Road, Hangzhou 310012, China

b Key Laboratory of Freshwater Biodiversity Conservation, Ministry of Agriculture and Rural Affairs,

Yangtze River Fisheries Research Institute, Chinese academy of Fishery Sciences, Wuhan, 430223, China

c Faculty of Fisheries Sciences, Hokkaido University, 3-1-1 Minato-cho, Hakodate, Hokkaido 041-8611,

Japan

d Liangzhu laboratory, Zhejiang University Medical Center, Hangzhou 310058, Zhejiang, China

Corresponding author at: Zhejiang Province Joint Key Laboratory of Aquatic Products Processing,

Institute of Seafood, Zhejiang Gongshang University, Hangzhou 310012, China.

E-mail addresses: dawei@mail.zjgsu.edu.cn (D. Meng)

Abstract

During the processing of sturgeon, large amounts of by-products, such as skin, fin, cartilage, and notochord, are produced. These by-products have not been effectively used, resulting in a serious waste of sturgeon resources. In this study, we aimed to obtain the collagen from these by-products and evaluate the fibril-forming characteristics of the collagen molecules and the antioxidant activity of the collagen peptides. The structural properties of pepsin-soluble collagen were analyzed by SDS-PAGE and FTIR. Collagen fibril-forming characteristics were detected by turbidity assay and SEM observation. The antioxidant activities of collagen peptides were determined by Hydroxyl and ABTS radical scavenging assays. SDS-PAGE results showed that the skin and fin collagens were characterized as type I collagen, and the cartilage and notochord collagens were characterized as type II collagen. Sturgeon type II collagens could only be self-assembled into fibrils at low phosphate ion concentration, whereas sturgeon type I collagens could be self-assembled into fibrils at long range of phosphate ion concentrations. The fibril-forming ability of sturgeon type I collagen was higher than that of porcine type I collagen. The fibril diameter of type I collagen was higher than that of type II collagen. The antioxidant activity of notochord and skin collagen peptides was higher than that of the other two collagen peptides. The results of this study will provide helpful information for the application of sturgeon collagen in the functional food and biomedical material industries. Meanwhile, it will promote the effective use of collagen from different sturgeon by-products.

Graphical abstract

Statement of Novelty

In China, more than 16,000 tons of female sturgeon are used for caviar production. After roe retrieval,

collagen-rich by-products, which are not suit for edible, will be produced during the processing of fish.

This work was the first to clarify and compare structural properties of collagen extracted from four

main by-products (fin, skin, notochord, cartilage) of sturgeon in one research. Furthermore, this work

was the first to discuss the biological properties of sturgeon collagen from high molecular collagen

fibril and low molecular collagen peptides, respectively. The results of this study will provide helpful

information of sturgeon collagens in different by-products. Meanwhile, according to its own functional

characteristics, different collagen will be used reasonably and effectively in a suitable field.

Introduction

Sturgeon is an economically valuable fish known for its caviar. Due to overfishing and destruction of

the living environment, since 1997 all wild sturgeons have been listed as critically endangered and

protected species by the International Union for Conservation of Nature [1]. To meet the demand for

caviar and reduce the pressure on wild sturgeon, aquaculture industry has developed rapidly in the past

20 years. The total global harvest of farmed sturgeon increased from 18,000 ton in 2003 to more than

102,000 ton in 2019 [2]. China is the biggest sturgeon farming and caviar producing country in the

world. In 2017, the aquaculture volume of sturgeon in China exceeded 80,000 tons, accounting for 85%

of the world's total production; the output of caviar exceeded 100 tons, accounting for 78% of the

world's total production [2, 3]. Currently, approx. 20% of China's total sturgeon production is the large

67   females that produces caviar.

68   Russian sturgeon *(Acipenser gueldenstaedti)* is one of species of sturgeon native to the sea area at

69   the junction of Asia and Europe [4]. In current, it is a commercial sturgeon species accounting for 10%

70   of the annual production of sturgeon in China [5, 6]. The main purpose of Russian sturgeon farming is

71   to produce caviar. Since it takes more than 10 years to obtain roe, Russian sturgeon is more expensive

72   to farm than other fishes, including hybrid sturgeon. After egg retrieval, these large fish bodies (over

73   1.5 meters) are divided into several parts for further processing. During the production process, huge

74   amounts of inedible by-products, such as head, skin, bone, fin, and viscera, are produced. These by-

75   products are not suitable for consumption and represent up to more than 70% of the total fish body. In

76   the past, sturgeon by-products were often discarded as waste or used as material for direct feeding in

77   aquaculture and raising of livestock and fur animals in China. As known, discarding these sturgeon by-

78   products will aggravate the problem of environmental pollution. The lack of efficient use of these by-

79   products other than caviar limits the profitability of aquaculture industry and leads to waste of fish

80   sources. Efficient utilization of these by-products will increase the value of Russian sturgeon, create

81   more economic benefits, and promote the development of sturgeon aquaculture. Meanwhile, it will

82   avoid wasting Russian sturgeon resources. Previous studies have shown that some sturgeon by-

83   products contained a variety of bioactive collagens [7, 8, 9].

84   Collagen is a main structural protein in the connective tissue of living organism [11]. *In vivo*,

85   collagen interacts with other components, such as proteoglycan and other proteins, to form a stable

86   network of fibrils. This fibrillar structure provides an appropriate growth environment for cells and

87   affects cellular functions [9]. *In vitro*, fibrillar collagen molecules can self-assemble into fibrils that

88   reassemble native tissue forms under suitable conditions [10]. Due to this special biological property,

89 collagen is widely used as biomedical materials to repair or replace damaged or diseased human tissues

90 and organs. In recent years, with the increasing demand for high value-added utilization of aquatic

91 waste, more and more researches on fish collagen have been conducted [9]. With no zoonotic risks and

92 religious restrictions, fish by-products are considered as a safe natural source of collagen [11, 12]. Our

93 recent studies have reported the biochemical characteristics and fibril-forming properties of collagen

94 from hybrid sturgeon (*Huso huso* × *Acipenser ruthenus*) skin, swim bladder, and notochord [7, 8, 13].

95 We found that different tissues contained different types of collagens and that there were significant

96 differences in the fibril-forming ability of collagen in tissues specific. For example, collagen extracted

97 from sturgeon swim bladder and skin was type I collagen, while collagen extracted from sturgeon

98 notochord was type II collagen [7, 8]. Although both swim bladder and skin collagen were type I

99 collagen, the fibril-forming ability and fibril morphology of two collagens were significant different

100 [13]. The *in vitro* fibril-forming ability is closely related to the application of collagen in biomedical

101 materials. In addition, the morphological characteristics of collagen fibrillar materials, including their

102 diameter, shape, and orientation, have a determining influence on the adhesion, alignment,

103 proliferation, and differentiation of anchorage-dependent cells [14]. Therefore, in order to utilize

104 collagens from different Russian sturgeon by-products, it is necessary to clarify and compare the

105 structural properties and fibril-forming properties of collagens in different tissues. To our knowledge,

106 no previous study has reported the *in vitro* fibril-forming properties of Russian sturgeon collagens.

107   On the other hand, low molecular collagen peptides attracted high attention of researchers because

108 of their various bioactivities, such as antioxidant, antihypertensive, antimicrobial, anticancer activities,

109 and so on [15]. Due to these bioactivities, collagen peptides are used as functional ingredient additives

110 in health foods and cosmetics. In aerobic organisms, reactive oxygen species (ROS) with a high

111   reaction activity, including hydroxyl radical, superoxide anion radical, hydrogen peroxide, and singlet

112   oxygen, are generated during the metabolism [16]. In general, cellular antioxidases, such as superoxide

113   dismutase, glutathione peroxidase, and catalase, can keep ROS in a state of balance [17]. Ultraviolet

114   irradiation, aging, stress, environmental deterioration, and other reasons can disrupt the balance, and

115   excess ROS in the body can induce enzyme inactivation, polysaccharide depolymerization, DNA

116   cleavage, and cell membrane destruction [17]. Till now, amounts of studies have been conducted on the

117   antioxidant activity of collagen peptides from fish tissues [18]. For sturgeon, some studies have

118   investigated the antioxidant activity of collagen peptides from their skin and cartilage [19, 20].

119   However, there was no study on the antioxidant activity of collagen peptides from notochord and fin.

120   Furthermore, the antioxidant activity of different types of collagen peptides, such as type I and II

121   collagen peptides, have never been compared in previous studies.

122   The aim of this study was to clarify the structural properties of collagen extracted from four main

123   by-products of Russian sturgeon, and to evaluate the fibril-forming characteristics of the four collagen

124   molecules and the antioxidant activity of the four collagen peptides. Firstly, we extracted pepsin-

125   soluble collagen from the four main by-products of fin, skin, backbone cartilage, and notochord in the

126   same method. Then, we evaluated *in vitro* fibril-forming properties of collagen molecules using

127   turbidity assay and SEM observation. Finally, we compared the antioxidant activities of collagen

128   enzymatic hydrolysates using ABTS and Hydroxyl radical-scavenging assays. The results of this study

129   will clarify the properties of collagen from the four main by-products and promote the efficient

130   utilization of collagen in different tissues of Russian sturgeon. Meanwhile, it will provide helpful

131   information for the application of Russian sturgeon collagen in the biomedical material and functional

132   food industries.

133 **Materials and methods**

134 **Isolation and purification of collagen**

135 The fin, skin, backbone, and notochord of the Russian sturgeon *(Acipenser gueldenstaedti)* after

136 spawning were obtained from the Sturgeon Biological Technology Co. Ltd. (Xinchang county,

137 Zhejiang province, China). The samples were washed with chilled tap water, and lyophilized in a freeze

138 dryer (FreeZone 2.5 L, American Labconco Co, Ltd, Kansas City, USA). The fat of backbone cartilage,

139 fin, and skin was removed over 24 h in anhydrous ethanol (two solution-changes) at 4 °C, with a

140 sample : solution ratio of 1:10 (w/v). Defatted samples and notochord sheath were cut into small pieces

141 for collagen extraction. Due to antigenic telopeptides existing at both ends of the collagen molecule,

142 acid-soluble collagen may not be suitable for direct use as biomaterials [21]. Pepsin can cleave the

143 peptides in the telopeptide region in extraction process [22]. In this study, we focused on pepsin-soluble

144 collagen from sturgeon by-products. Isolation and purification progress of pepsin-soluble collagen were

145 performed according to the procedures reported by our previous method [8, 23]. Porcine skin and

146 bovine cartilage collagens were used to compare the structural properties and biological activities of

147 Russian sturgeon collagens. The samples were obtained from Fuyang Jiuxian Beef Slaughtering Co.

148 Ltd. (Hangzhou, Zhejiang province, China). The pepsin-soluble collagen extraction method was the

149 same as above.

150 **Sodium dodecyl sulfate-polyacrylamide gel electrophoresis (SDS-PAGE)**

151 SDS-PAGE was performed according to the method of Laemmli [24]. The lyophilized collagen was

152 dissolved in pH 2.0 HCl at a concentration of 1 mg/ml. The collagen samples were mixed at a ratio of

153 1:1(v/v) with sample buffer (0.5 M Tris-HCl buffer, pH 6.8, with 4% SDS and 20% glycerol)

154 containing 10% β-mercaptoethanol. The mixed solution was boiled for 3 min. Ten micrograms of

155 mixture were loaded onto each lane. Electrophoresis was performed at 15 mA for the stacking gel and

156 25 mA. Collagen molecule electrophoresis was running with the 8% running gel, collagen enzymatic

157 hydrolysates was running with the 15% running gel. After electrophoresis, the gel was stained for 30

158 min with a 0.1% Coomassie Brilliant Blue R250 solution and de-stained with a mixture of 20%

159 methanol, 5% acetic acid, and 2.5% glycerin.

160 **Fourier-transform infrared (FTIR) spectroscopy analysis**

161 FTIR spectroscopy of collagen was recorded with an infrared spectrophotometer (Nicolet iS10, Thermo

162 Scientific, Madison, USA). The collagen powder was ground together with potassium bromide (w/w

163 1:200), and then pressed into a 1 mm pellet for measurement in the spectra range of 500-4000 cm^{-1}.

164 The potassium bromide powder was used as the background.

165 **Solubility of collagen in different pH**

166 The solubility of collagen was measured using the method proposed by Atef et al [25]. with a slight

167 change. Dry collagen was dissolved in aqueous solutions with different pH (2, 4, 6, 8, 10, 12) to

168 3mg/ml. The collagen solution was shake for 12 h at 21 °C. Then, each collagen solution was

169 centrifugated at 20,000 ×g for 20 min at 4 °C, the protein concentration of the supernatant was

170 measured by Lowry method [26], using bovine serum albumin as a standard. The solubility of collagen

171 was defined as the percentage of the collagen concentration in the solution, ie, the solubility of collagen

172 at different pH conditions.

173 **Collagen fibril formation *in vitro***

174 The fibril formation process of collagen was evaluated by the method of Meng et al [8]. Lyophilized

175 collagen was dissolved in pH 2.0 HCl solution to 0.3% (w/v). The collagen solution was mixed with a

176 Na-phosphate buffer (PB) solution (pH 7.4), having a Na-phosphate concentration of 45, 90, and 180

177 mM, respectively. The collagen solution/PB ratio was set to 1:2 (v/v), which resulted in a final PB

178 concentration of 30 ,60, and 120 mM, respectively. The mixed solution was place into a quartz cuvette,

179 and the subsequent fibril formation at 21°C was monitored by measuring increased turbidity via optical

180 absorbance at 320 nm, using a spectral monitor (Evolution 60 s, Thermo fisher scientific, Waltham,

181 USA). The fibril formation of skin and fin collagen was monitored for 1 h. The fibril formation of

182 backbone and notochord collagen was monitored for 10 h.

183 **Morphology of collagen fibrils**

184 The microstructure of fin and skin collagen fibrils was observed using scanning electron microscope

185 (SEM; Sigma 500, Carl Zeiss Ltd, Germany), as previously described in Meng et al [8]. Collagen fibrils

186 were formed using the same conditions as described above. Sample suspensions were centrifuged at

187 20,000 $\times g$ for 20 min at 4 °C to obtain precipitates of collagen fibrils. The fibrils were fixed with 2.5%

188 (v/v) glutaraldehyde in phosphate buffer (pH 7.4) for 3 h at room temperature, rinsed with phosphate

189 buffer to remove the fixative, dehydrated with a graded series of ethanol solutions, and then soaked in

190 two 30-min changes of t-butyl alcohol solution. Finally, collagen fibrils were freeze-dried in a t-butyl

191 alcohol solution with a freeze-drying device and coated with gold-platinum using an auto fine coater

192 (JFC-1600; JEOL Ltd.). After the SEM observations, digital images of the sample were taken, and the

193 diameters of 100 randomly selected fibrils were determined using the software ImageJ. The

194 measurements were performed three times using different photographs.

195 **Degree of fibril formation**

196 The fibril formation degree was determined followed by the method of Zhang et al [7]. After fibril

197 formation, the mixture was centrifugated at 20,000 $\times g$ for 20 min at 4 °C, the protein concentration of

198 the supernatant was measured by Lowry method [26], using bovine serum albumin as a standard. The

199   degree of fibril formation was defined as the percentage of the decrease of collagen concentration in

200   the solution, which meant the percentage of collagen molecules that formed the fibrils. The fibril

201   formation degree was detected after completion of fibril formation for each sample.

202   **Enzymatic hydrolysis of collagen**

203   Purified collagens were soaked in distilled water with a sample/solution ratio of 1:60 (w/v) at 60 °C for

204   1 h for gelatinization. Papain was used to hydrolyze purified collagens with a concentration of 2.5%

205   (w/w) for 4 h at 50 °C. The reaction was terminated by boiling samples for 10 min. The reaction

206   solution was filtered with cellulose acetate membrane filter (pore size 0.45 μm) remove the

207   unhydrolyzed residues. Then, all hydrolysates were lyophilized and stored at −30 °C until use. The

208   percentage of dry weight of collagen hydrolysate in comparison with dry weight of the initial collagen

209   was calculated as the collagen peptide yield.

210   **Hydroxyl scavenging activity of collagen peptides**

211   Hydroxyl radical scavenging activity was determined according to the method of Pan et al. [27].

212   Briefly, a 1,10-phenanthroline solution (1.0 ml, 1.865 mM) was mixed with 2 ml of the sample

213   solution, and then $FeSO_4 \cdot 7H_2O$ solution (1.0 ml, 0.75 mM) was pipetted into the mixture. The reaction

214   was initiated by adding 1.0 ml of H_2O_2 (0.01% v/v). After incubation at 37°C for 60 min, the

215   absorbance was measured at 536 nm against a reagent blank. The reaction solution without antioxidants

216   was used as a negative control, and the mixture without H_2O_2 was used as the blank. Vitamin C (Vc)

217   was used as positive control. The hydroxyl radical scavenging activity was calculated according to Eq.

218   1:

219   Scavenging activity (%) = [(As − An) / (Ab − An)] × 100%

220   where As, An, and Ab are the absorbance values at 536 nm of the sample, negative control, and blank

221   after the reaction, respectively.

222   **ABTS radical scavenging activity of collagen peptides**

223   The ABTS radical scavenging activity was determined by the method of Re et al. [28]. In brief, ABTS

224   radical cation was generated by mixing the ABTS stock solution (7 mM) with potassium persulfate

225   (2.45 mM). The mixture was left in the dark at room temperature for 16 h. The ABTS radical solution

226   was diluted in 5 mM phosphate buffered saline at pH 7.4 to an absorbance of 0.7 at 734 nm. One

227   milliliter of diluted ABTS radical solution was mixed with 1 ml of different concentrations of samples.

228   Ten minutes later, the absorbance was measured at 734 nm against the corresponding blank. Vc was

229   used as positive control. The ABTS radical scavenging activity of samples was calculated according to

230   Eq. 2:

231   Scavenging activity (%) = [(Ac – As) / Ac] × 100%

232   where As and Ac are the absorbances with and without a sample.

233   **Statistical analysis**

234   Each experiment was replicated three times. The data of collagen solubility, fibril formation degree,

235   and radical scavenging activity were expressed as means ± standard errors.

236   **Results and Discussion**

237   **SDS-PAGE**

238   The α-chain pattern of collagens was shown in Fig. 1. Fin and skin collagens (Lane 1 and 2) contained

239   two α-chains (approx. 120 kDa and 110 kDa) as the major constitutes and a small amount of β-chain.

240   The major α-chains at 120 kDa and 110 kDa were attributed to the α1(I) or α3(I), and α2(I) of type I

241   collagen, respectively. The molecular weight of sturgeon type I collagen was a little lower than that of

242   porcine skin type I collagen, but they had the similar α-chain pattern (Lane 5). The α-chain pattern of

243   skin collagen in this study was consistent with our previous study on the skin collagen of hybrid

244   sturgeon *(Huso huso × Acipenser ruthenu*s) [8]. The band of α1(I) in fin collagen was much thicker

245   than that in skin collagen, indicating differences in the molecular structure of fin and skin collagens.

246   Nagai et al. reported that the sea-bass fin collagen was type I collagen, which only contained a single α

247   band [29]. Liu et al. found that bighead carp fin collagen had both α1(I) and α2(I) in a ratio of 2.12

248   [30]. It is well known that type I collagen comprises two α1(I) chains and one α2(I) chain in a ratio of

249   2:1, and its molecular form is $[\alpha1(I)]_2\alpha2(I)$ [31]. Meanwhile, Saito et al. reported that a heterotrimer of

250   type I collagen containing three non-identical α-chains, α1(I) α2(I) α3(I), was found in the skin and

251   muscle collagen of rainbow trout [32]. Since α3(I) and α1(I) had similar molecular weight, they could

252   not be separated by electrophoresis. Low α2(I) was detected by electrophoresis in SDS-PAGE result

253   indicated that the molecular structure of sturgeon fin collagen might contain more triple helical

254   molecules with α-chain patterns of $\alpha1[I]_3$, $\alpha1[I]_2\alpha3[I]$, $\alpha1[I]\alpha3[I]_2$, and $\alpha3[I]_3$. Zhang et al. reported that

255   the ratio of α1/α2 gene expression was higher in the fin than in the skin of Amur sturgeon *(Acipenser*

256   *schrenckii)*. Although different sturgeon species might have different gene expression, the gene

257   expression results was consistent with the SDS-PAGE results of this study [33].

258   The notochord collagen (Lane 3) contained a single major band at approx. 130 kDa, which was

259   the characteristic of type II collagen α-chain [8]. β-chain was not detected in the notochord collagen. A

260   slight high molecular weight band above major α-chain was presumed to be type IX or XI collagen

261   [34]. The α-chain composition of notochord collagen was consistent with that of bovine cartilage

262   collagen (Lane 6). These results were consistent with the α-chain properties of Bester sturgeon *(Huso*

263   *huso × Acipenser ruthenus*) notochord collagen [7]. It suggested that the α-chain pattern of notochord

264   collagen was independent of sturgeon species.

265   The cartilage collagen (Lane 4) contained three α-chains (approx. 130 kDa, 120 kDa and 110 kDa)

266   as the major constituents and a small amount of β-chain. The major α-chain at 130 kDa was attributed

267   to the α1(II) of type II collagen. The other two α-chains (approx.120 kDa and 110 kDa) were

268   corresponded to α1(I) and α2(I) of type I collagen. This result was consistent with the conclusion that

269   type II collagen was the main collagenous component in cartilage tissue [35]. The reason for the

270   presence of type I collagen in backbone was thought to be cartilage ossification. Ossification is a

271   process by which bone form in soft tissues, such as cartilage [36]. Zhang et al. showed that ossification

272   of the spine cartilage was observed in hybrid sturgeon *(H. huso × A. ruthenus)* [37]. Leprévost et al.

273   also reported that bone was deposited around the spine cartilage of Siberian sturgeon *(Acipenser*

274   *Baerii)* [38]. As known, type I collagen constituted approx. 95% of total collagen in bone [39]. The

275   exact proportion of type I collagen in sturgeon backbone was not known from this study. It might be

276   related to the degree of cartilage ossification. Leprévost et al. found that the bone thickness on the

277   cartilage varied with the region of cartilage and the age of sturgeon [38]. In addition, Zhang et al.

278   reported that gene of ascol1α1 (Col I) and ascol2α1 (Col II) were expressed in sturgeon vertebral

279   cartilage [40]. It demonstrated the presence of type I collagen in sturgeon backbone cartilage by

280   molecular analyses. The results of α-chain patterns in this research were consistent with this finding.

281   Mizuta et al. and Luo et al. reported that type I collagen was the major collagenous components in

282   the vertebral cartilage of White sturgeon *(Acipenser transmontanus)* and Siberian sturgeon *(Acipenser*

283   *baeri)* [41, 42]. Liang et al. and Zhu et al. reported that the pepsin-soluble collagens extracted from the

284   cartilage of Hybrid sturgeon *(Acipenser schrencki × Huso dauricus)* and Amur sturgeon *(Acipenser*

285   *schrenckii)* were type II collagen [34, 43]. The differences in α-chain patterns among sturgeon species

286   were thought to be caused by different extraction processes. In our previous study, we found that type

287 II collagen was more difficult to extract than type I collagen by the same extraction method [8]. In this

288 research, we stopped the collagen extraction process until there was no residue in the extract. It allowed

289 complete extraction of type I and type II collagen molecules. Since the purification process of two

290 collagens was same, the pepsin-soluble cartilage collagen purified in this study contained both two type

291 collagens. Furthermore, during collagen purification process, the NaCl concentration used might be

292 another reason for obtaining different types of collagens. Because, during salting out process, different

293 type of collagens could be precipitated in a biological tissue using different concentrations of NaCl

294 [44]. In fact, we found that in the current studies, the NaCl concentrations used to isolate the sturgeon

295 cartilage collagen were all different in these studies [34, 41, 42, 43].

296 **FTIR spectroscopic analysis**

297 The FTIR spectra was presented in Fig. 2. showing the intact triple helical structure in collagens.

298 According to Plepis et al [45], the ratio of absorbance of amide III to peak between 1400 to 1454 cm^{-1}

299 wavelength is close to 1.0, indicating that the triple helical structure of collagen is intact. In this study,

300 the ratios of fin, skin, notochord, and cartilage collagen were 0.97, 1.05, 1.01 and 0.99, respectively.

301 The ratios of porcine skin and bovine cartilage collagen were 1.00 and 0.99, respectively. It indicated

302 that the complete triple helical structure was retained in all collagens. Otherwise, the main

303 characteristic absorption peaks of collagen contained amide A, amide B, amide I, amide II, and amide

304 III. The amide A band of fin, skin, notochord, and cartilage collagen was 3326.36, 3290.14, 3293.34,

305 and 3283.22 cm^{-1}, respectively. The amide A band of porcine skin and bovine cartilage collagen was

306 3304.35 and 3300.23 cm^{-1}, respectively. Muyonga et al. reported that the absorption band of amide A,

307 associated with N-H stretching vibration [46]. The amide B band of fin, skin, notochord, and cartilage

308 collagen was observed at 2931.10, 2947.55, 2933.68, and 2927.90 cm^{-1}, respectively. The amide B

band of porcine skin and bovine cartilage collagen was observed at 2935.82 and 2933.76 cm^{-1},

respectively. It was associated with the asymmetrical stretching of CH$_2$. The amide I band frequencies

from 1600 to 1700 cm^{-1} were mainly related to carbonyl group stretching vibrations and were

characteristic of the secondary coil structure [47]. The amide I bond of fin, skin, notochord, and

cartilage collagen was observed at 1658.96, 1661.35, 1631.48, and 1633.41 cm^{-1}, respectively. The

amide I bond of porcine skin and bovine cartilage collagen was observed at and 1628.50 and 1630.56

cm^{-1}, respectively. This observation confirmed the formation of hydrogen bonds between N-H stretch,

where the C-O residues were responsible for stabilizing the triple helical structure [46]. The amide II

and III of fin, skin, notochord, and cartilage collagen were observed at 1453.92, 1452.80, 1547.60, and

1541.81 cm^{-1}; 1239.56, 1239.76, 1238.08, and 1236.15 cm^{-1}, respectively. The amide II and III of

porcine skin and bovine cartilage collagen were observed at 1548.20 and 1546.15; 1237.33 and

1237.32 cm^{-1}, respectively. The amide II band corresponded to N-H bending vibration, and the amide

III band represented C-H stretching [47]. The FTIR spectra of all collagens were consistent with the

structural properties of collagen.

Solubility of collagen

Collagen molecules have the minimum solubility at their isoelectric point and therefore suitable for

fibril formation *in vitro* [48]. To discuss the suitable pH condition for fibril-forming, the influence of

pH on collagen molecule solubility was investigated as shown in Fig. 3. For fin collagen (Fig. 3-a), the

highest solubility appeared at pH 2. The solubility significantly decreased with pH value increasing to

6. The minimum solubility of fin collagen appeared at pH value between 6 and 8. It indicated that the

isoelectric point of fin collagen was between pH 6 to 8. A slight increase in solubility was found at pH

values of 8 to 12. When the pH value increased to 12, the solubility of fin collagen was dramatically

331 rose to 63.0%. The reason for the high solubility of collagen on the alkaline side might be due to the pH

332 being far from its isoelectric point. For skin collagen (Fig. 3-b), it solubilized to a greater extent in the

333 acidic pH range from 2 to 3. The solubility significantly decreased with pH value increased to 8. The

334 minimum solubility of skin collagen appeared at pH values between 6 to 8. It indicated that the

335 isoelectric point of skin collagen was between pH 6 to 8. When the pH value increased to 10, the

336 solubility of skin collagen rose sharply to 51.1%. It suggested that the solubility of skin collagen was

337 more sensitive to pH change to alkaline side than that of fin collagen.

338 Cartilage collagen (Fig. 3-d) solubilized to a greater extent in the acidic pH range from 2 to 3. The

339 solubility significantly decreased with pH value increasing to 10. The minimum solubility of cartilage

340 collagen appeared at pH values between 8 and 10. It indicated that the isoelectric point of cartilage

341 collagen was between pH 8 and 10. When the pH value increased to 12, the solubility of cartilage

342 collagen was dramatically rose to 78.3%. For notochord collagen (Fig. 3-c), the highest solubility

343 appeared at pH 2. The solubility of notochord collagen was more sensitive to pH change than that of

344 cartilage collagen. As pH value increased to 6, the solubility sharply decreased to 0.57%. A slight

345 increase in solubility was found at alkaline pH values of 8 to 10. It suggested that the isoelectric point

346 of notochord collagen was between pH 6 and 8. Like cartilage collagen, the solubility of notochord

347 collagen increased rapidly with increasing pH value to 12. The solubility results indicated that there

348 were differences in the molecular properties and conformations of the four collagens. Furthermore,

349 amino acid composition is also a non-negligible factor that affects the protein isoelectric point, which

350 in turn affects protein solubility [49].

351 The solubility of collagen with changes in pH may play a crucial role in its extraction method. So

352 far, many studies have discussed the effect of different pH values from 1 to 10 on type I collagen

353 solubility [31]. In this study, we found for the first time that the solubility of sturgeon collagen

354 increased, when the pH was increased to 12. It suggested that part of the collagen molecules could be

355 dissolved in alkaline solution. In our previous study, we reported that sturgeon collagen was lost during

356 the alkaline pretreatment [8]. This result was consistent with the results of collagen solubility,

357 indicating that the alkali-soluble collagen was presented in the sturgeon by-products. Therefore,

358 although alkaline pretreatment can improve collagen extraction efficiency, the conditions of the

359 alkaline pretreatment need to be considered to avoid more collagen loss.

360 **Collagen fibril formation *in vitro***

361 In general, collagen fibril-forming process is divided into three phases: lag phase (no turbidity

362 changes), growth phase (turbidity increasing), and plateau phase (turbidity stabilization) [13]. The

363 progression of fin and skin collagen fibril-forming at different phosphate ion concentrations was shown

364 in Fig. 4 (a and b). When the phosphate ion concentration of solution was 30 mM, the turbidity curves

365 of the two collagens were similar, with no lag phase. At 120 mM phosphate ion concentration, the

366 turbidity of both two collagens did not change. It indicated that collagen fibrils were not formed at 120

367 mM phosphate ion concentration. The effect of phosphate ion concentration on skin collagen fibril-

368 forming were consistent with our previous studies [13]. Significant differences between fin and skin

369 collagen turbidity curves occurred at 60 mM phosphate ion concentration. At this condition, the

370 turbidity curve of fin collagen contained a long lag phase and a smooth growth phase. The plateau

371 phase was not observed after 1 h reaction. For skin collagen, after a short lag phase, a steep growth

372 phase was observed with a rapid increase in turbidity value to near 2. In our previous study, we

373 demonstrated that high phosphate ion concentration inhibited the fibril-forming of sturgeon type I

374 collagen [13]. The inhibitory effect of phosphate ion concentration on fin collagen fibril-forming was

375   more significant than that of skin collagen. During collagen fibril-forming, linear aggregation of

376   collagen molecules occurred in the lag phase to form subfibrillar units. These subfibrillar units

377   aggregate laterally in the growth phase to form fibrils [50]. The turbidity curve results indicated that, at

378   high phosphate ion concentration, fin collagen needed longer time to form subfibrillar units and was

379   more difficult to self-assemble into thick fibrils than skin collagen. The rate of fibril-forming was

380   mainly controlled by intermolecular interaction between collagen molecules [51]. The progression of

381   porcine skin type I collagen fibril-forming at different phosphate ion concentrations was shown in Fig.

382   4-c. The turbidity changes of porcine skin type I collagen only appeared at 30 mM phosphate ion

383   concentration. The turbidity increasing of porcine skin type I collagen was much slower than sturgeon

384   type I collagen. It indicated that the fibril-forming ability of sturgeon type I collagen was higher than

385   that of porcine skin type I collagen.

386   Type II collagen took more time to self-assemble into fibrils than type I collagen. Notochord and

387   cartilage collagens could only form fibril at 30 mM phosphate ion concentration (Fig. 4 c and d). As

388   phosphate ion concentration increased to 60 mM, the turbidity of both two collagens did not change. It

389   indicated that type II collagen could only form fibrils at low phosphate ion concentration compared to

390   type I collagen. No lag phase with no changes in turbidity was observed in the two turbidity curves. It

391   was because the fibril formation speed was too fast that no lag phase was detected in both two type II

392   collagens. The progression of bovine cartilage type II collagen fibril-forming at different phosphate ion

393   concentrations was shown in Fig. 4-f. The turbidity change trends of sturgeon and bovine type II

394   collagens under different phosphate ion concentration conditions were similar. It suggested that

395   sturgeon and bovine type II collagens had similar fibril-forming ability under the same phosphate ion

396   concentration condition. However, the turbidity curves of bovine and rat type II collagens have been

397   reported to have a longer lag phase during fibril formation [10, 52]. Long lag phase might be due to the

398   different ionic environments in solution. The initial turbidity of cartilage collagen started at 0.53, and

399   then the turbidity curve increased slowly with reaction time. The final turbidity of cartilage collagen

400   ended at 0.70. The initial turbidity of notochord collagen was 0.38, and then the turbidity curve rose

401   rapidly in the first 100 min. After that, the rate of turbidity growth slowed down and the final turbidity

402   ended at 0.78. The turbidity change trend of notochord collagen in this study was consistent with that

403   of Bester sturgeon notochord collagen [8]. The difference in absorbance values came from the amount

404   of collagen added. Comparing to cartilage collagen, the notochord collagen formed fibril with a longer

405   growth phase. It suggested that the fibril formation speed of cartilage collagen was faster than that of

406   notochord collagen. Our previous study reported that collagen fibril lateral aggregation occurred during

407   the growth phase, and the final turbidity value reflected fibril thickness [13]. This result indicated that

408   the fibril diameter of notochord collagen was larger than that of cartilage collagen. Different

409   conformations and molecular structures of collagens might be responsible for their different fibril-

410   forming properties.

411   **Fibril formation degree**

412   The degree of fin and skin collagen fibril formation was assessed after 1 h, and the results were shown

413   in Fig. 5 (a and b). When phosphate ion concentration was 30 mM, the fibril formation degree of fin

414   collagen and skin collagen were $93.34 \pm 0.23\%$ and $94.93 \pm 0.11\%$, respectively. When phosphate ion

415   concentration was 60 mM, the fibril formation degree of fin collagen and skin collagen were $90.15 \pm$

416   1.07% and $94.05 \pm 0.71\%$, respectively. At the same phosphate ion concentration, the fibril formation

417   degree of skin collagen was slightly higher than that of fin collagen. The fibril formation degree of both

418   two collagens decreased with increasing phosphate ion concentration. This trend was consistent with

419   Bester sturgeon swim bladder and skin type I collagens [13]. The fibril formation degree of skin

420   collagen at 60 mM phosphate ion in this research was much higher than that of Bester sturgeon skin

421   collagen [13]. Different species of sturgeon were thought to be responsible for different skin collagen

422   fibril formation processes.

423   The degree of notochord and cartilage collagen fibril formation was assessed by 10 h

424   fibrillogenesis, and the results were shown in Fig. 5 (c). Both notochord and cartilage collagens showed

425   high fibril formation degree with values of 95.13 ± 0.15% and 98.32% ± 0.03%, respectively. It meant

426   that almost all collagen molecules re-assembled into collagen fibrils after 10 h reaction. The degree of

427   fibril formation in notochord collagen was consistent with that of Bester sturgeon notochord collagen

428   [13].

429   **Fibril diameter and morphology**

430   SEM images of fin and skin collagen fibrils formed after incubation for 1 h were shown in Fig. 6, while

431   the diameter distributions of the fibrils were shown in Fig. 8 (a and b). For both collagens, fibril

432   diameter became thicker with increasing phosphate ion concentration in solution. This trend was

433   consistent with the sturgeon swim bladder type I collagen reported in our previous study [13].

434   Increasing the magnification of the SEM observation in this study showed the fibrillar morphology

435   more clearly than our previous results. At 30 mM phosphate ion concentration, the thick fibrils

436   appeared in both fin and skin collagen fibrils. Many oriented long fibrils were interlaced with thin

437   fibrils. The mean fibril diameter for fin and skin collagen was 58.0 and 60.7 nm, respectively. At a

438   phosphate ion concentration of 60 mM, the mean fibril diameter for fin and skin collagen was 154.9

439   and 209.0 nm, respectively. The range of the fibril diameter increased significantly comparing with at

440   30 mM phosphate ion concentrations. There were no fibrils less than 50 nm in diameter throughout the

441   fibrillar structure, and the maximum diameter of fin and skin collagen fibrils were 334 and 477 nm,

442   respectively. The fibril morphology and diameter results suggested that the phosphate ion concentration

443   had a certain influence on the morphology of sturgeon fin collagen fibrils. However, unlike skin

444   collagen, fin collagen could not be formed thick fibrillar structure even at high phosphate ion

445   concentration. Sturgeon fin collagen could only form fine fibrils *in vitro*. From Fig. 6 (a-1 and a-2 60

446   mM PB), we found a special dense network structure interlaced with the fibrils and attached to the

447   surface of the fibrils. These special structures formed steric hindrance and inhibited the aggregation of

448   collagen fibrils into thick fibrils. It might be the reason for that fin collagen fibrils were much thinner

449   than skin collagen fibrils. From this study, the exact composition of these dense network structures was

450   not known. Combined with the discussion in the SDS-PAGE section, we speculated that these special

451   structures might be composed of other collagens. Histochemistry method and molecular analyses will

452   be used to demonstrated this hypothesis in our further study. Another characteristic of fibrils under this

453   condition was that a transverse periodic band pattern structure could be observed on fin and skin

454   collagen fibrils. It is well known that the 67 nm D-periodic band pattern is the characteristic of the

455   natural type I collagen fibril *in vivo* [53]. To investigate whether these periodic band patterns resemble

456   the structure of native collagen fibrils *in vivo*, detailed observation of the fibrils using transmission

457   electron microscopy is required in further studies.

458   In Fig. 6 (b-2 60 mM PB), the ends of the thick fibrillar structure were clearly observed in the skin

459   collagen fibrils (as shown by the white arrow). The tip of the fusiform structure consisted of several

460   skin collagen fibrils. The coarse fibrils were formed by random parallel convergence of several fine

461   fibrils. This process occurred during the growth phase, and many long fibrils accumulated into thick

462   fibrils, resulting in a rapid increase in the turbidity of the solution. Our previous study showed that the

463   thick fusiform structure was found in the swim bladder collagen fibrils at 60 mM phosphate ion

464   concentration, but the structure of the tip of the fusiform was not observed clearly [13]. In this research,

465   we increased observation magnification of SEM and clearly observed the structural properties of the

466   fusiform fibril.

467   SEM images of the notochord and cartilage collagen fibrils after 10 h of incubation were shown in

468   Fig. 7. The diameter distributions of the fibrils were shown in Fig. 8 (c and d). The mean fibril

469   diameters of notochord and cartilage collagens were 52.0 nm and 37.3 nm, respectively. The diameter

470   distribution of notochord collagen fibrils ranged from 11 to 157 nm. The fibrils with diameters less than

471   75 nm accounted for 83.3% of the total fibrils. The diameter distribution of cartilage collagen fibrils

472   ranged from 9 to 127 nm, and the fibrils with diameters less than 50 nm accounted for 77.2% of the

473   total fibrils. Overall, notochord collagen fibrils contained more thick fibrils than cartilage collagen

474   fibrils. Weiss et al. reported that type II collagen fibrils in human articular cartilage have diameters in

475   the range of 40-80 nm [54]. It suggested that the re-assembled fibrils of sturgeon notochord and

476   cartilage type II collagens had a similar thickness degree to native human cartilage fibrils.

477   The unordered, net-like appearance of fine fibrils exhibited in both notochord and cartilage

478   collagen fibrils (Fig 8 a-1 and b-1). Comparing to cartilage collagen fibrils, notochord collagen fibrils

479   contained more thick fusiform structure interwoven with fine fibrils (white arrows in Fig 8 b-2 and b-

480   3). These special fusiform structures enable notochord collagen fibrils had a higher fibril diameter

481   distribution than cartilage collagen fibrils. As shown by white arrows in Fig. 7 b-3, the thick fusiform

482   structure was formed by the accumulation of many fine fibrils. This result was consistent with the

483   result of turbidity curve. During the long growth phase of notochord collagen, more fine fibrils

484   accumulated into thick fibrils. The formation of fibrils with different morphology might be due to the

485　presence of a small amount of type I collagen in cartilage collagen. In our previous study, we

486　demonstrated that the amino acid compositions were different between type I and type II collagens [8].

487　Therefore, the molecular conformations of two types collagens were also different. The formation of

488　collagen fibrils *in vitro* was a highly regular self-assembly process. The presence of type I collagen

489　might cause steric hindrance to the regular self-assembly process of type II collagen molecules. Lapiere

490　et al. reported that the addition of other collagens reduced the lateral aggregation of type I collagen

491　fibrils, resulting in the formation of fine fibril networks [55]. Adachi & Hayashi also reported that type

492　V collagen restricted the growth of type I collagen fibrils to thick fibrils *in vitro* [56]. To our best

493　knowledge, till now there was no similar studies on type II collagen fibril formation. Here we

494　hypothesis that the presence of type I collagen will affect the fibril-forming process and fibril

495　morphology of cartilage type II collagen. In our further study, pure type I and type II collagens will be

496　used to demonstrate this hypothesis.

497　**Yields and molecular distribution of collagen peptides**

498　Papain was a plant-derived protease for food processing. In our recent study, Li et al demonstrated that

499　papain hydrolysates of skate cartilage had higher antioxidant activity and lower molecular weight than

500　other protease hydrolysates (such as trypsin, chymotrypsin, and pepsin) [57]. In addition, papain is

501　comparatively less expensive than the other proteolytic enzymes [57]. Considering the production

502　efficiency and the cost for large-scale production, we used papain to treat four sturgeon collagens in

503　this study. The yields of collagen peptides for fin, skin, notochord, and cartilage were 78.8%, 99.1%,

504　74.2%, and 89.2%, respectively. The SDS-PAGE of collagen peptides was shown in Fig. 9. Notochord

505　collagen peptide was smeared after CBB staining with no clear bands, whereas other collagen peptides

506　showed several bands at molecular weight above 17 kDa. Cartilage collagen peptide showed two bands

507   at molecular weight above 24 kDa. It suggested that notochord collagen peptide had more low

508   molecular peptides compared to the other three collagen peptides, while cartilage collagen peptide had

509   more high molecular weight peptides. Except for notochord collagen peptide, the other three collagen

510   peptides had a smearing area on the SDS-PAGE. The smearing area was an aggregate of collagen

511   peptides with similar molecular weight. It also indicated that the molecular weight of notochord

512   collagen peptide was lower than that of the other three collagen peptides.

513   **Antioxidant activity of collagen peptides**

514   Among the ROS generated in an animal body, the hydroxyl radical is the primary active oxygen species

515   with the strongest reactivity. Therefore, the scavenging of hydroxyl radicals is one of the most effective

516   defense mechanisms of a living body against various diseases. Hydroxyl radical scavenging activity of

517   the collagen peptides was summarized in Fig. 10-a. The activities of all collagen peptides increased in

518   concentration-dependent manners. At the same concentration, the Hydroxyl radical scavenging activity

519   of the four collagen peptides was notochord > skin > fin > bovine cartilage > porcine skin > cartilage.

520   The antioxidant activity of notochord collagen peptide was higher than that of Vc, when the sample

521   concentration was 5 mg/mL.

522   ABTS radical scavenging activity of collagen peptides was shown in Fig. 10-b. All collagen

523   peptides showed ABTS radical scavenging activity in a dose-dependent manner. At the same

524   concentration, the ABTS radical scavenging activity order of the four collagen peptides was skin >

525   notochord > fin > bovine cartilage > cartilage > porcine skin. Although the molecular weight of

526   notochord collagen peptide was lower than that of skin collage peptides, the antioxidant activity of skin

527   collagen peptide was higher than that of notochord collagen peptides. It suggested that the antioxidant

528   activity of collagen peptides was not only related to the molecular weight of peptides. The results of

529 two free radical scavenging activities also showed that the antioxidant activity of collagen peptides was

530 directly related to collagen type. Comparing with the other two sturgeon by-products, the skin and

531 notochord was more suitable for producing antioxidant collagen peptide.

532 **Conclusions**

533 The present study was the first to clarify the collagen structural characteristics of collagens, which

534 extracted from four Russian sturgeon by-products. Meanwhile, the biological properties of the four

535 collagens were compared through the fibril formation ability of the collagen molecule and the antioxidant

536 activity of the collagen peptide. The α-chain pattern results indicated that the main collagen of fin and

537 skin was type I collagen, and the main collagen of notochord and cartilage was type II collagen. The

538 solubility results of collagen at different pH suggested that the isoelectric points of the skin, fin, and

539 notochord collagens were approx. in the pH range of 6 to 8. Notochord and cartilage type II collagen

540 could only self-assemble into fibril at low phosphate ion concentration condition, while skin and fin type

541 I collagen could self-assemble into fibril at a wide range of phosphate ion concentration. The fibrillar

542 morphology of type I collagen was more diversified than that of type II collagen. Under the same

543 hydrolysis of papain, the molecular weight of notochord collagen peptide was lower than that of the other

544 three collagen peptides. The antioxidant activity of notochord and skin collagen peptide was better than

545 that of the other collagen peptides. Since there is no previous study on the utilization of Russian sturgeon

546 collagen, this study will provide basic data for the application of Russian sturgeon collagen in the food

547 and biomedical material industries. Meanwhile, the effective utilization of collagen will be a feasible

548 way to increase the value of Russian sturgeon by-products.

References

1. Birstein, V. J., Bemis, W. E., Waldman, J. R.: The threatened status of acipenseriform species: A summary. Environ. Biol. Fish. **48**, 427-435 (1997).

2. Tavakoli, S., Luo, Y. K., Regenstein, J. M., Daneshvar, E., Bhatnagar, A., Tan, Y. Q., Hong, H.: Sturgeon, Caviar, and Caviar Substitutes: From Production, Gastronomy, Nutrition, and Quality Change to Trade and Commercial Mimicry. Rev. fish. Sci. Aquac. **29**, 753-768 (2021).

3. Bronzi, P., Chebanov, M., Michaels, J. T., Wei, Q. W., Rosenthal, H., Gessner, J.: Sturgeon meat and caviar production: Global update 2017. J. Appl. Ichthyol. **35**, 257-266 (2019).

4. Hurvitz, A., Jackson, K., Degani, G., Levavi-Sivan, B.: Use of endoscopy for gender and ovarian stage determinations in Russian sturgeon *(Acipenser gueldenstaedtii)* grown in aquaculture. Aquaculture. **270**, 158-166 (2007).

5. Chen, Y. W., Cai, W. Q., Shi, Y. G., Dong, X. P., Bai, F., Shen, S. K., Jiao, R., Zhang, X. Y., Zhu, X.: Effects of different salt concentrations and vacuum packaging on the shelf stability of Russian sturgeon *(Acipenser gueldenstaedti)* stored at 4 °C. Food. Control. **109**, 106865 (2020).

6. Meng, D. W., Leng, X. Q., Zhang, Y., Luo, J., Du, H., Takagi, Y., Dai, Z. Y., Wei, Q. W.: Comparation of the structural characteristics and biological activities of chondroitin sulfates extracted from notochord and backbone of Chinese sturgeon *(Acipenser sinensis)*. Carbohydr. Res. **522**, 108685 (2022).

573   7. Zhang, X., Ookawa, M., Tan, Y. K., Ura, K., Adachi, S., Takagi, Y.: Biochemical characterisation and

574   assessment of fibril-forming ability of collagens extracted from Bester sturgeon *Huso huso* ×

575   *Acipenser ruthenus*. Food. Chem. **160**, 305-312 (2014).

576   8. Meng, D. W., Tanaka, H., Kobayashi, T., Hatayama, H., Zhang, X., Ura, K., Yunoki, S., Takagi, Y.:

577   The effect of alkaline pretreatment on the biochemical characteristics and fibril-forming abilities of

578   types I and II collagen extracted from bester sturgeon by-products. Int. J. Biol. Macromol. **131**, 572-

579   580 (2019).

580   9. Strueuli, C.: Extracellular matrix remodelling and cellular differentiation. Curr. Opin. Cell. Biol. **11**,

581   634-640 (1999).

582   10. Silver, F. H., Freeman, J. W., Seehra, G. P.: Collagen self-assembly and the development of tendon

583   mechanical properties. J. Biomech. **36**, 1529-1553 (2003).

584   11. Kim, S. K., Mendis, E.: Bioactive compounds from marine processing byproducts – A review. Food.

585   Res. Int. **39**, 383-393 (2006).

586   12. Alves, A. L., Marques, A. L. P., Martins, E., Silva, T. H., Reis, R. L.: Cosmetic potential of marine

587   fish skin collagen. Cosmetics. **4**, 4040039 (2017).

588   13. Meng, D. W., Li, W., Ura, K., Takagi, Y.: Effects of phosphate ion concentration on in-vitro

589   fibrillogenesis of sturgeon type I collagen. Int. J. Biol. Macromol. **148**, 182-191 (2020).

590   14. Curtis, A. S. G., Clark, P.: The effects of topographic and mechanical properties of materials on cell

591   behavior. Crit. Rev. Biocompat. **5**, 343-362 (1990).

592   15. Ahmed, M., Verma, A. K., Patel, R.: Collagen extraction and recent biological activities of collagen

593   peptides derived from sea-food waste: A review. Sustain. Chem. Pharm. **18**, 100315 (2020).

594   16. Taghvaei, M., Jafari, S.M., Mahoonak, A. S., Nikoo, A.M., Rahmanian, N., Hajitabar, J., Meshginfar,

595 N.: The effect of natural antioxidants extracted from plant and animal resources on the oxidative

596 stability of soybean oil. LWT-Food. Sci. Technol. **56**, 124-130 (2014).

597 17. Mahapatra, S., Chakraborty, S., Majumdar, S., Bag, B., Roy, S.: Eugenol protects nicotine-induced

598 superoxide mediated oxidative damage in murine peritoneal macrophages *in vitro*. Eur. J. Pharmacol.

599 **623**, 132-140 (2009).

600 18. Zhao, X. C., Zhang, X. J., Liu, D. Y.: Collagen peptides and the related synthetic peptides: A review

601 on improving skin health. J. Funct. Foods. **86**, 104680 (2021).

602 19. Sheng, Y., Qiu, Y. T., Wang, Y. M., Chi, C. F., Wang, B.: Novel antioxidant collagen peptides of

603 Siberian Sturgeon *(Acipenser baerii)* cartilages: the preparation, characterization, and

604 cytoprotection of H_2O_2-damaged human umbilical vein endothelial cells (HUVECs). Mar. Drugs.

605 **20**, 325 (2022).

606 20. Nikoo, M., Benjakul, S., Xu, X. M.: Antioxidant and cryoprotective effects of Amur sturgeon skin

607 gelatin hydrolysate in unwashed fish mince. Food. Chem. **181**, 295-303 (2015).

608 21. Clowacki, J., Mizuno, S.: Collagen scaffolds for tissue engineering. Biopolymers. **89**, 338-344 (2007).

609 22. Nalinanon, S., Benjakul, S., Visessanguan, W., Kishimura, H.: Use of pepsin for collagen extraction

610 from the skin of bigeye snapper *(Priacanthus tayenus)*. Food. Chem. **104**, 593-601 (2007).

611 23. Meng, D. W., Li, W., Leng, X. Q., Takagi, Y., Dai, Z. Y., Du, H., Wei, Q. W.: Extraction of chondroitin

612 sulfate and type II collagen from sturgeon *(Acipenser gueldenstaedti)* notochord and

613 characterization of their hybrid fibrils. Process. Biochem. **124**, 180-188 (2023).

614 24. Laemmli, U. K.: Cleavage of structural proteins during the assembly of the head of bacteriophage T4.

615 Nature. **277**, 680–685 (1970).

616 25. Atef, M., Ojagh, S. M., Latifi, A. M., Esmaeili, M., Udenigwe, C. C.: Biochemical and structural

617   characterization of sturgeon fish skin collagen (Huso huso). J. Food. Biochem. **44**, e13256 (2020).

618   26. Lowry, O. H., Rosebrough, N. J., Farr, A. L., R. Randall, J.: Protein measurement with the folin

619   phenol reagent. J. Biol. Chem. **193**, 265–275 (1951).

620   27. Pan, X., Zhao, Y., Hu, F., Wang, B.: Preparation and identification of antioxidant peptides from

621   protein hydrolysate of skate *(Raja porosa)* cartilage. J. Funct. Foods. **25**, 220-230 (2016).

622   28. Re, R., Pellegrini, N., Proteggente, A., Pannala, A., Yang, M., Rice-Evans, C.: Antioxidant activity

623   applying an improved ABTS radical cation decolorization assay, Free Radic. Biol. Med. **26**, 1231-

624   1237 (1999).

625   29. Nagai, T.: Characterization of collagen from Japanese sea bass caudal fin as waste material. Eur.

626   Food. Res. Technol. **218**, 424-427 (2004).

627   30. Liu, D. S., Liang, L., Regenstein, J. M., Zhou, P.: Extraction and characterisation of pepsin-solubilised

628   collagen from fins, scales, skins, bones and swim bladders of bighead carp *(Hypophthalmichthys*

629   *nobilis)*. Food. Chem. **133**, 1441-1448 (2012).

630   31. Foegeding, E. A., Lanier, T. C., Hultin, H. O.: Food. Chem, ed. by Fennema OR. New York, Marcel

631   Dekker Inc, pp. 902-906 (1996).

632   32. Saito, M., Takenouchi, Y., Kunisaki, N., Kimura, S.: Complete primary structure of rainbow trout

633   type I collagen consisting of α1 (I) α2 (I) α3 (I) heterotrimers. Eur. J. Med. Chem. **268**, 2817-2827

634   (2001).

635   33. Zhang, X., Adachi, S., Ura, K., Takagi, Y.: Properties of collagen extracted from Amur sturgeon

636   *Acipenser schrenckii* and assessment of collagen fibrils in vitro. Int. J. Biol. Macromol. **137**, 809-

637   820 (2019).

638   34. Liang, Q. F., Wang, L., Sun, W. H., Z. Wang, B., Xu, J. M., Ma, H. L.: Isolation and characterization

639   of collagen from the cartilage of Amur sturgeon *(Acipenser schrenckii)*. Process. Biochem. **49**, 318-

640   323 (2014).

641   35. Li, S. W., Prockop, D. J., Helminen, H., Fassler, R., Lapvetelainen, T., Kiraly, K., Peltarri, A.,

642   Arokoski, J., Lui, H., Arita, M.: Transgenic mice with targeted inactivation of the Col2 alpha 1 gene

643   for collagen II develop a skeleton with membranous and periosteal bone but no endochondral bone.

644   Gene. Dev. **9**, 2821-2830 (1995).

645   36. Medici, D., Olsen, B. R.: The role of endothelial- mesenchymal transition in heterotopic ossification.

646   J. Bone. Miner. **27**, 1619-1622 (2012).

647   37. Zhang, X., Shimoda, K., Ura, K., Adachi, S., Takagi, Y.: Developmental structure of the vertebral

648   column, fins, scutes and scales in bester sturgeon, a hybrid of beluga *Huso huso* and sterlet

649   *Acipenser ruthenus*. J. Fish. Bio. **81**, 1985-2004 (2012).

650   38. Leprévost, A., Azaïs, T., Trichet, A., Sire, J. Y.: Vertebral development and ossification in the siberian

651   sturgeon *(Acipenser Baerii)*, with new insights on bone histology and ultrastructure of vertebral

652   elements and scutes. The. Anatomical. Record. **300**, 437-449 (2017).

653   39. Viguet-Carrin, S., Garnero, P., Delmas, P. D.: The role of collagen in bone strength. Osteoporosis. Int.

654   **17**, 319-336 (2006).

655   40. Zhang, X., Azuma, N., Hagihara, S., Adachi, S., Ura, K., Takagi, Y.: Characterization of type I and II

656   procollagen α1chain in Amur sturgeon *(Acipenser schrenckii)* and comparison of their gene

657   expression. Gene. **579**, 8-16 (2016).

658   41. Mizuta, S., Asano, C., Yokoyama, Y., Taniguchi, M.: Molecular species of collagen in muscular and

659   vertebral parts of white sturgeon Acipenser transmontanus. Fisheries. Sci. **78**, 399-406 (2012).

660   42. Luo, Q. B., Chi, C. F., Yang, F., Zhao, Y. Q., Wang, B.: Physicochemical properties of acid-and

661   pepsin-soluble collagens from the cartilage of Siberian sturgeon. Environ. Sci. Pollut. R. **25**, 31427-

662   31438 (2018).

663   43. Zhu, L. L., Li, J. W., Wang, Y. C., Sun, X., Li, B. F., Poungchawanwong, S., Hou, H.: Structural

664   feature and self-assembly properties of type II collagens from the cartilages of skate and sturgeon.

665   Food. Chem. **331**, 127340 (2020).

666   44. Sato, K., Ohashi, C., Ohtsuki, K., Kawabata, M.: Type V collagen in trout *(Salmo gairdneri)* muscle

667   and its solubility change during chilled storage of muscle. J. Agri. Food. Chem. **39**, 1222-1225

668   (1991).

669   45. Plepis, A. M. D. G., Goissis, G., Gupta, D. D.: Dielectric and pyroelectric characterization of anionic

670   and native collagen. Polym. Eng. Sci. **36**, 2932-2938 (1996).

671   46. Muyonga, J. H., Cole, C. G. B., Duodu, K. G.: Characterisation of acid soluble collagen from skins

672   of young and adult Nile perch *(Lates niloticus)*. Food. Chem. **85**, 81-89 (2004).

673   47. Veeruraj, A., Arumugam, M., Balasubramanian, T.: Isolation and characterization of thermostable

674   collagen from the marine eel-fish *(Evenchelys macrura)*. Process. Biochem. **48**, 1592-1602 (2013).

675   48. Li, Y. P., Douglas, E. P.: Effects of various salts on structural polymorphism of reconstituted type I

676   collagen fibrils. Colloids. Surf. B. **112**, 42-50 (2013).

677   49. Patrickios, C. S.: Polypeptide amino acid composition and isoelectric point: 1. A closed-form

678   approximation. J. Colloid. Interf. Sci. **175**, 256-260 (1995).

679   50. Kalbitzer, L., Pompe, T.: Fibril growth kinetics link buffer conditions and topology of 3D collagen I

680   networks. Acta. Biomater. **67**, 206-214 (2018).

681   51. Shi, L. F., Tian, H. H., Wang, Y. X., Hao, G. X., Chen, J., Weng, W. Y.: Effect of pH on properties of

682   golden pompano skin collagen-based fibril gels by self-assembly *in vitro*. J. Sci. Food. Agr. **100**,

683   4801-4807 (2020).

684   52. Birk, D. E., Silver, F. H.: Collagen fibrillogenesis in vitro: comparison of types I, II, and III. Arch.

685   Biochem. Biophys. **235**, 178-185 (1984).

686   53. Kemp, N. E.: Banding pattern and fibrillogenesis of ceratotrichia in shark fins. J. Morph. **154**, 187-

687   204 (1977).

688   54. Weiss, C., Rosenberg, L., Helfet, A. J.: An ultrastructural study of normal young adult human articular

689   cartilage. J. Bone. Joint. Surg. Am. **50**, 663-674 (1968).

690   55. Lapiere, C. M., Nusgens, B., Pierard, G. E.: Interaction between collagen type I and type III in

691   conditioning bundles organization. Connect. Tissue. Res. **5**, 21-29 (1977).

692   56. Adachi, E., Hayashi, T.: In vitro formation of hybrid fibrils of type V collagen and type I collagen

693   limited growth of type I collagen into thick fibrils by type V collagen. Connect. Tissue. Res. **14**,

694   257-266 (1986).

695   57. Li, W., Kobayashi, T., Meng, D. W., Miyamoto, N., Tsutsumi, N., Ura, K., Takagi, Y.: Free radical

696   scavenging activity of type II collagen peptides and chondroitin sulfate oligosaccharides from by-

697   products of mottled skate processing. Food. Biosci. **41**, 100991 (2021).

698

699   **Statements and Declarations**

700   **Funding**

704   **Competing Interests**

705   The author declares that he has no conflict of interest.

706   **Author Contribution**

707   All authors had read and agreed with the published version of the manuscript. Dawei Meng:

708   Conceptualization, Methodology, Data curation, Investigation, Writing-original draft. Qiwei Wei:

709   Supervision. Prof. Yasuaki Takagi: Methodology, Writing-review & Editing. Prof. Zhiyuan Dai:

710   Resources. Yan Zhang: Methodology. All authors read and approved the final manuscript.

711   **Data availability**

712   Not applicable.

713

714   **Fig. 1** SDS-PAGE of collagen. M: Molecular weight marker; Lane 1: fin collagen; Lane 2: skin collagen;

715   Lane 3: notochord collagen; Lane 4: backbone cartilage collagen; Lane 5: porcine skin collagen;

716   Lane 6: bovine cartilage collagen

717   **Fig. 2** Infra-red spectra of the sturgeon (a) fin collagen; (b) skin collagen; (c) notochord collagen; (d)

718   backbone cartilage collagen: (e) porcine skin collagen; (f) bovine cartilage collagen

719   **Fig. 3** Solubility of the sturgeon (a) fin collagen; (b) skin collagen; (c) notochord collagen; (d) backbone

720   cartilage collagen at different pH

721   **Fig. 4** Fibril formation in vitro by (a) fin collagen; (b) skin collagen; (c) porcine skin collagen; (d)

722   notochord collagen; (e) backbone cartilage collagen; (f) bovine cartilage collagen measured by

723   optical absorbance at 320 nm with different PB buffer concentration (30, 60, 120 mM)

724   **Fig. 5** The degree of fibril formation of collagen. (a) fin collagen in 30 mM and 60 mM PB buffer; (b)

725   skin collagen in 30 mM and 60 mM PB buffer; (c) notochord and backbone cartilage collagen in 30

726   mM PB buffer

727   **Fig. 6** Scanning electron micrographs of sturgeon fin and skin collagen fibrils in 30 mM and 60 mM PB

728   buffer. (a) fin collagen; (b) skin collagen. Scale bars: (1) 10 μm; (2) 1 μm. White arrow in b-2 60

729   mM PB: The fusiform structure at the tip of skin collagen fibril

730   **Fig. 7** Scanning electron micrographs of sturgeon notochord and backbone cartilage collagen fibrils in

731   30 mM PB buffer. (a) notochord collagen; (b) backbone cartilage collagen. Scale bars: (1) 2 μm; (2)

732   2 μm; (3) 0.2 μm. White arrow: Thick fusiform structure of notochord collagen fibril

733   **Fig. 8** Diameter distribution of sturgeon collagen fibril (a) fin collagen fibril in 30 mM and 60 mM PB

734   buffer; (b) skin collagen fibril in 30 mM and 60 mM PB buffer; (c): notochord collagen fibril in 30

735   mM PB buffer; (d) backbone cartilage collagen fibril in 30 mM PB buffer

736   **Fig. 9** SDS-PAGE of sturgeon collagen peptides. M: molecular maker; Lane 1: fin collagen peptide; Lane

737   2: skin collagen peptide; Lane 3: notochord peptide; Lane 4: backbone cartilage peptide.

738   **Fig. 10** Hydroxyl (a) and ABTS (b) radical scavenging activities of collagen peptides.

Four main sturgeon by-products

Cartilage Notochord

Acipenser gueldenstaedti

Skin Fin

Collagen extraction
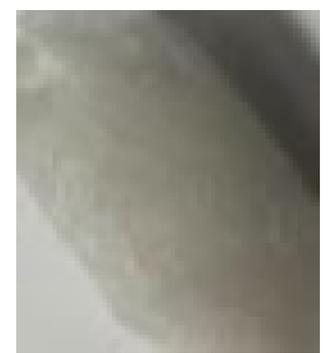
Undenatured collagen (Lyophilized sample)

Structural characteristics

α-chain pattern

Triple helical structure

Biological properties

High molecular collagen fibril

Fibril forming ability Fibrillar morphology

Low molecular collagen peptides

MW distribution Antioxidant activity

Fig.1

Fig.2

Fig.3

Fig.4

Fig.5

Fig.6

a-1 30 mM PB | a-2 30 mM PB
a-1 60 mM PB | a-2 60 mM PB
b-1 30 mM PB | b-2 30 mM PB
b-1 60 mM PB | b-2 60 mM PB

Fig.7

Fig.8

Fig.9

Fig.10